

Original Research

Contrast Enrichment of Spinal Cord MR Imaging Using a Ratio of T1-Weighted and T2-Weighted Signals

Masatoshi Teraguchi, MD,^{1*} Hiroshi Yamada, MD, PhD,¹ Munehito Yoshida, MD, PhD,¹ Yoshiaki Nakayama, MD,² Tomoyoshi Kondo, MD, PhD,² Hidefumi Ito, MD, PhD,² Masaki Terada, MD, PhD,³ and Yoshiki Kaneoke, MD, PhD⁴

Purpose: We aimed to assess if the T1-weighted (T1w)/T2-weighted (T2w) signal ratio could be used to improve image contrast in MR spinal cord imaging.

Materials and Methods: T1w and T2w cervical spinal cord MR images were acquired from 23 normal subjects using 3 Tesla (T) MR scanner. In addition, a multiple sclerosis patient, and a cervical spondylotic myelopathy patient were evaluated. White matter (WM) and gray matter (GM) signal intensities were measured for each image (T1w, T2w, and T1w/T2w) for seven cervical segments in each subject to calculate the contrast. Age-related changes in signal intensity were assessed at each location (lateral column, anterior column, dorsal column, and GM) for each image. Additionally, the imaging results of two subjects with spinal diseases and the controls were numerically compared.

Results: The contrast between the WM and GM in the T1w/T2w ratio image was approximately twice as much as that in the T1w and T2w images (mean \pm SD = 1.8 \pm 0.4). The signal intensity ratio was related to age. For both clinical patients, the signal intensities were significantly lower in the lesion areas in the ratio images.

Conclusion: The T1w/T2w ratio images demonstrated increased image contrast compared with T1w and T2w images alone and, reduced inter-individual signal intensity differences.

Key Words: contrast; magnetic resonance imaging; ratio; spinal cord; T1 weighted image; T2 weighted image

J. Magn. Reson. Imaging 2014;40:1199–1207.

© 2013 Wiley Periodicals, Inc.

MRI HAS BEEN used successfully for the diagnosis of various spinal cord diseases since the early 1980s. Fast spin echo (FSE) and gradient recalled echo (GRE) are the most commonly used sequences because they provide relatively good lesion contrast and anatomical resolution of spinal cord structures (1). However, it is still difficult to clearly discriminate gray matter (GM) from white matter (WM) in the spinal cord on routine spinal images acquired in clinical practice, despite distinct histological differences between the tissues (2,3). In addition, some intradural-extramedullary lesions cannot be differentiated from intramedullary lesions (4). Moreover, because the signal intensity of MRI varies with body size and its position relative to the coil (5–7), the changes are not always related to specific pathologic processes (8,9). Previously, several MRI-based approaches to improve the detection of pathological changes in the spinal cord have been investigated using the motion properties (diffusion) of water molecules (10–12) or relaxation times to measure the myelin water fraction (13–17).

Recently, Glasser and Van Essen showed that the ratio of the signal intensity in T1-weighted (T1w) MRI to the signal intensity in T2-weighted (T2w) MRI was sensitive to subtle differences in myelin content within the gray matter of the cerebral cortex (18). Although it is not certain to what extent the signal intensity of the T1w/T2w ratio image is related to the myelin content, the T1w/T2w ratio eliminates the signal intensity bias related to receiver coil sensitivity. Additionally, it increases the image contrast if the ratio is calculated using a pair of voxels at exactly the same anatomical location for both T1w and T2w MRI.

MATERIALS AND METHODS

Participants

Twenty-three healthy volunteers (15 men and 8 women; ages, 22–86 years; mean \pm standard deviation (SD) = 44.5 \pm 22.5) were recruited for this study. Additionally, two subjects with spinal myelopathies were enrolled to compare their spinal images with those of

¹Department of Orthopedics, Graduate School of Wakayama Medical University, Wakayama, Japan.

²Department of Neurology, Graduate School of Wakayama Medical University, Wakayama, Japan.

³Wakayama-Minami Radiology Clinic, Wakayama, Japan.

⁴Department of System Neurophysiology, Graduate School of Wakayama Medical University, Wakayama, Japan.

Contract grant sponsor: 2013 Wakayama Medical Award for Young Researchers.

*Address reprint requests to: M.T., Department of Orthopedics, Graduate School of Wakayama Medical University, 811-1 Kimiidera, Wakayama 641-8509, Japan. E-mail: m-tera@wakayama-med.ac.jp

Received December 5, 2013; Accepted September 11, 2013.

DOI 10.1002/jmri.24456

View this article online at wileyonlinelibrary.com.

the control: One was a 39-year-old man who was diagnosed with multiple sclerosis (MS) 7 years prior. At the time of the experiment, he had muscle weakness and spasticity predominantly in both lower extremities (right side dominant). The Romberg sign was positive. We did not detect any brain lesions in this subject, except for transient bilateral low visual acuity. The other subject was a 77-year-old man who underwent a laminoplasty for cervical spondylotic (CS) myelopathy 5 years prior. His gait was spastic and the Romberg sign was positive. He had some paresthesia in both hands and a right-side dominant diminished tendon reflex. This study was approved by the Clinical Research Ethics Board of our institution, and all subjects gave written informed consent before the study began.

MRI Data Acquisition

Two different MR images (see below) were acquired for each subject's cervical spinal cord on a 3 Tesla (T) MRI (Philips Medical Systems, Best, The Netherlands) using a 16-channel coil (SENSE Neurovascular coil 16). Each subject wore a Sternal Occipital Mandibular Immobilizer (SOMI) brace modified for MRI acquisition to minimize spontaneous movements of the head and neck. Three-dimensional (3D) T1w fast field gradient echo MR images were acquired with the following parameters: repetition time (TR) = 6.5 ms, echo time (TE) = 3.1 ms, 10° flip angle, field of view (FOV) 256 mm, matrix 256 mm × 256 mm, number of slices = 100, slice thickness = 2 mm, and axial (transverse) slice orientation. The resulting voxel size was 1 × 1 × 2 mm, and the acquisition time was 6 min 47 s. Next, 3D T2w turbo spin echo MR images were acquired with the following parameters: TR = 3200 ms, TE = 93 ms, 90° flip angle, FOV 256 mm, matrix 256 mm × 256 mm, number of slices = 100, slice thickness = 2 mm, and axial slice orientation. The resulting voxel size was 1 × 1 × 2 mm, and the acquisition time was 6 min 14 s. For both acquisitions, the SENSE algorithm (19) was used with a reduction factor of 1.8 and 1.5 for T1w and T2w, respectively.

Data Analysis

T1w/T2w ratio images were created from the magnitude images of the T1w and T2w acquisitions of each subject using in-house software developed in MATLAB (MathWorks, Natick, MA). In this study, the signal intensity of the T1w images was simply divided by the signal intensity of the T2w images at the same location, as determined from the original image coordinates. The T1w/T2w ratio erases the effect of the reception bias field (b) and increases the signal intensity related to pathological changes (x) as described by the following equation (18):

$$T1w/T2w = x * b / ((1/x) * b) = x^2$$

The segmental cervical spinal cord level was determined by its relative location to the cervical vertebrae in each subject. Thirty-three axial segmental images were chosen out of 100 images for each subject, which included all of the images from the cervical seg-

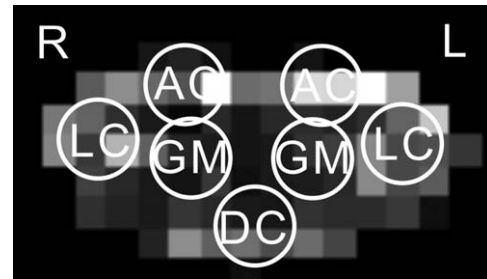


Figure 1. Signal intensity measurements. Using the original spatial resolution (1 × 1 mm) axial image of the T1w/T2w ratio, mean signal intensities were determined at seven locations (within a radius of 2 mm) that were determined visually for each segment.

ments with a 2-mm separation between adjacent images. For each axial image, the signal intensities were measured at seven locations that were related to the left and right lateral columns (LC), anterior columns (AC), single dorsal column (DC), and the left and right GM from 1 × 1 mm image slices (Fig. 1). For illustrative purposes, the images were resampled to 0.25 × 0.25 mm voxels using bicubic interpolation and 2D Gaussian spatial filtering. Each location was visually determined using the T1w/T2w ratio images at a high resolution (0.25 × 0.25 mm), which clearly delineated the GM and LC, AC, and DC, illustrating the so-called 'butterfly' shape, and the mean signal intensity of the voxels within a 2-mm radius were calculated. Additionally, the mean signal intensities for the T1w and T2w images were automatically calculated using voxels at the same location.

Axial images of the cervical spinal cord at the C4 level for each image type (T1w, T2w, and T1w/T2w) were made in the original 1 × 1 mm horizontal resolution images. These axial images were resampled at a high resolution (0.25 × 0.25 mm) using MATLAB. Additionally, to compare the T1w/T2w ratio image with stained spinal cord tissue, the spinal cord tissue at the C3, C5, and C7 levels was extirpated at autopsy. The tissues were obtained from the cervical cord at autopsy from an 83-year-old Japanese woman who died of pontine hemorrhage. They were fixed for several weeks in 10% neutral formalin, then the C3, C5, and C7 spinal cord levels were confirmed by counting nerve roots by two neuropathologists, resected and embedded in paraffin. Procedures involving use of human material were performed in accordance with ethical guidelines set by Kyoto University. The sample was stained with Kluver-Barrera stain. They were first resampled at a resolution of 1 × 1 mm and then resampled at 0.25 × 0.25 mm and Gaussian filtered using MATLAB.

The mean contrast between the WM locations (LC, AC, and DC) and GM (mean value across bilateral GM) was calculated using the following equation:

$$\text{Contrast (\%)} = 100 \times |I_w - I_g| / (I_w + I_g)$$

where I_w is the signal intensity of the WM (LC, AC, and DC) and I_g is the mean signal intensity of the bilateral GM.

The mean contrast was also assessed between each WM (LC, AC, and DC) location and mean GM value for

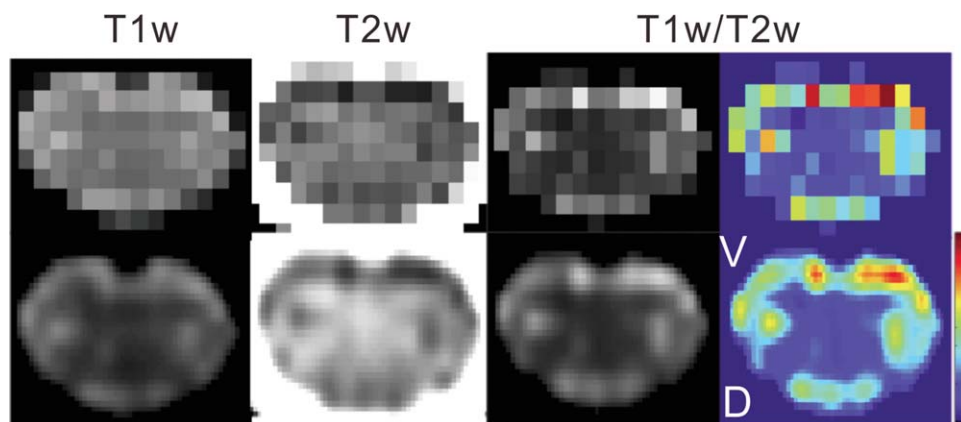


Figure 2. Comparison of the ratio images with the original MR images. The original resolution (1×1 mm) image (top) and the high resolution (0.25×0.25 mm) images for the T1w, T2w, and T1w/T2w ratio MRIs (bottom) are shown for the same cervical segment (C4) in one representative healthy subject. Contrast between the GM and WM is the highest for the T1w/T2w ratio images. The scale for each image is 10–90%.

all locations in the seven segments of the control subjects and for each image type (T1w, T2w, and T1w/T2w). Furthermore, the significance of the differences in mean contrast between the T1w/T2w ratio image and the T1w or T2w images were assessed for all locations by using a paired t-test with a Bonferroni correction.

Furthermore, using Pearson's correlation coefficient, we assessed the changes in signal intensity with age at each location (LC, AC, DC, and GM) at the C4 level for each image type (T1w, T2w, and T1w/T2w).

To check the reproducibility of the signal intensity measurement, the scan was acquired twice from nine healthy subjects (three women, aged 22–86 years). Six locations (signal intensity of the bilateral AC, LC, single DC, and the mean signal intensity of the bilateral GM) in seven segments from nine subjects were determined visually within a radius of 2 mm by using the T1w/T2w ratio images and using both measurements. Forty-two values from one subject were used to check the reproducibility of the measurement of each subject. The first signal intensity measurement at six locations in seven segments was performed by MT,

and the second measurement of the same six locations in seven segments was performed by H.Y. Kendall's coefficient of concordance was used to assess the significance of the reproducibility.

Finally, we verified that signal intensity changes were due to pathological changes by using the signal intensities in the T1w/T2w ratio images from the 39-year-old MS patient and the 77-year-old CS myelopathy patient. The T1w/T2w ratio intensities were plotted as a graph with the normal range between the broken lines (± 2 SD), which was estimated using the values from the controls (22–45 years of age). Because the signal intensity was inversely related to the age, each subject's normal range was adjusted using linear interpolation.

RESULTS

Contrast Increase Using the T1w/T2w Ratio

The axial images of the cervical spinal cord at the C4 level for one subject are shown in Figure 2. Even in the original 1×1 mm horizontal resolution image, it

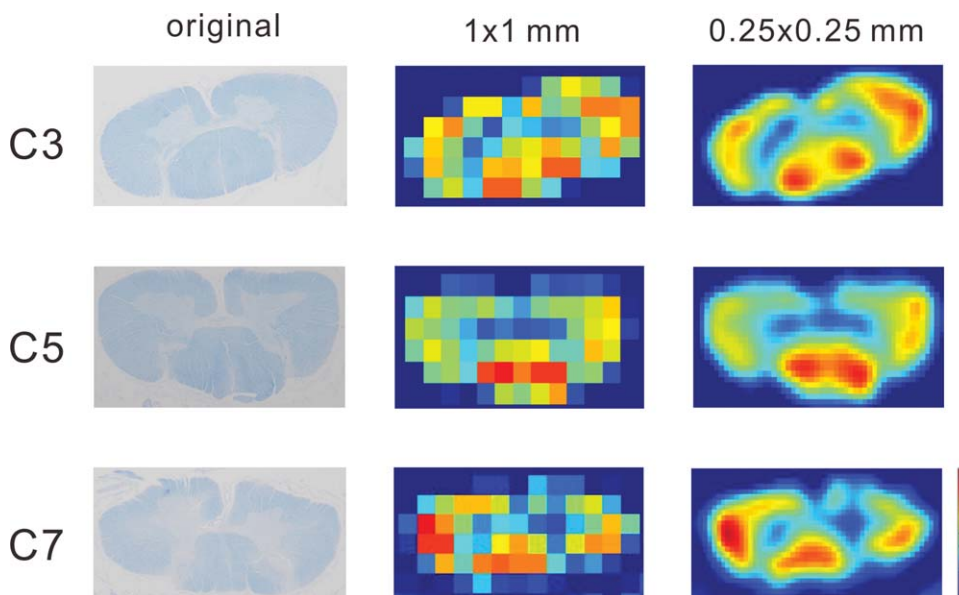


Figure 3. Spinal cord tissue at the C3, C5, and C7 levels. The spinal cord tissues at the C3, C5, and C7 levels were stained with Kluver-Barrera stain. They were first resampled at a resolution of 1×1 mm and then resampled at 0.25×0.25 mm and Gaussian filtered using MATLAB. (right side image).

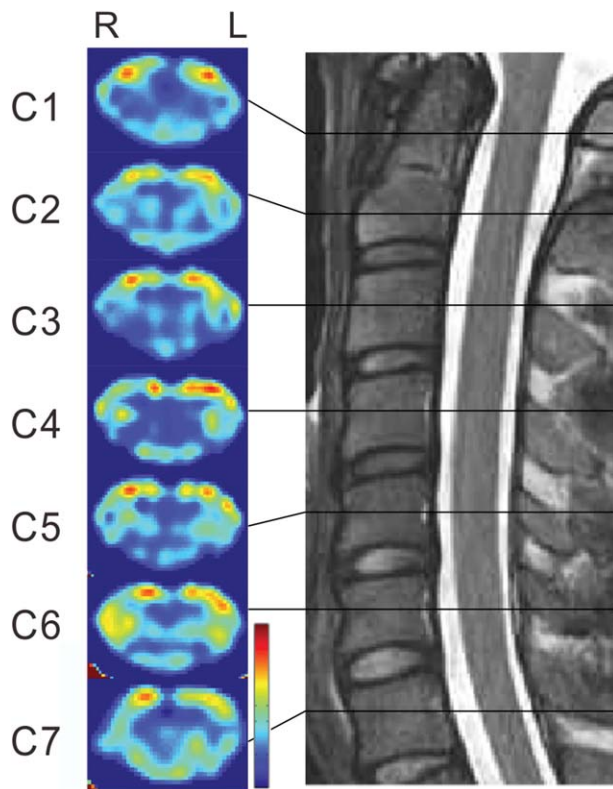


Figure 4. T1w/T2w ratio images at each cervical vertebral level. The right side of the figure shows the sagittal cervical T2w MR images. Axial T1w/T2w ratio images at each vertebral level (C1–C7) are shown on the left side of the figure (ventral at the top). High contrast between the GM and WM is seen at all cervical segments, but the so-called “butterfly” shape is the clearest at C4. The scale is 10–90% for each image.

is apparent that the contrast between the central GM and the peripheral WM is the highest for the T1w/T2w ratio image. The color T1w/T2w ratio image with high resolution (0.25×0.25 mm) clearly delineates the GM, illustrating the so-called “butterfly” shape.

We compared the T1w/T2w ratio image with the resampled image from the spinal cord tissue visually at the C3, C5, and C7 levels (Fig. 3). The signal intensity was different in each individual, but the color image from the T1w/T2w ratio image and the resampled image were similar in terms of distinction between the WM and GM, presenting a clear “butterfly” shape. In addition, the percentage in increase of the mean contrast between the LC and GM at three segments was 2.83%, and those between the AC and GM and between the DC and GM were 3.78% and 2.99%, respectively.

As shown in Figure 4, high contrast between the GM and WM was seen for all cervical segments, although the contrast was apparently related to the segmental level, with higher contrast observed in higher segments.

Figure 5 shows the mean contrast between the WM locations (LC, AC, and DC) and the GM (the mean value across the bilateral GM). Because no significant difference was observed between the right and left AC and LC contrast values, the averaged values are shown. Contrast was the highest at all locations and segmental levels in the T1w/T2w ratio images at approximately twice that of the T1w and T2w images. In addition, the contrast appeared to decrease as the segmental level increased.

Figure 6 shows that the mean contrast between the LC and GM for the T1w/T2w ratio images was 1.9 times larger than the mean contrast for the T1w images, and the values between the AC and GM and between the DC and GM were similar (2.2 and 1.9 times, respectively). The contrast increases in the T2w images were also similar, except for between the DC and GM values, which was 1.5 times. Additionally, the percentage in increase of the mean contrast between the LC and GM at seven segments was 6.38%, and those between the AC and GM and between the DC and GM were 6.01% and 3.51%, respectively.

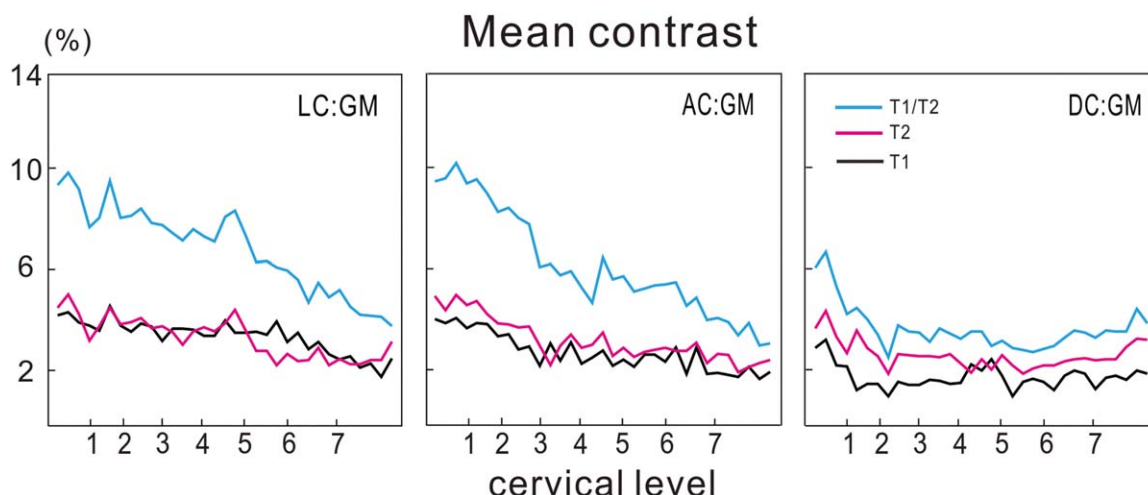


Figure 5. Mean contrast between each WM location and GM. Contrast for all locations at each segment level was the highest in the T1w/T2w ratio images, and the contrast decreased as the segmental level increased. The contrast for the T1w/T2w ratio images was approximately twice that of the T1w and T2w images. No significant difference in the contrast between the T1w and T2w images was observed for any of the locations.

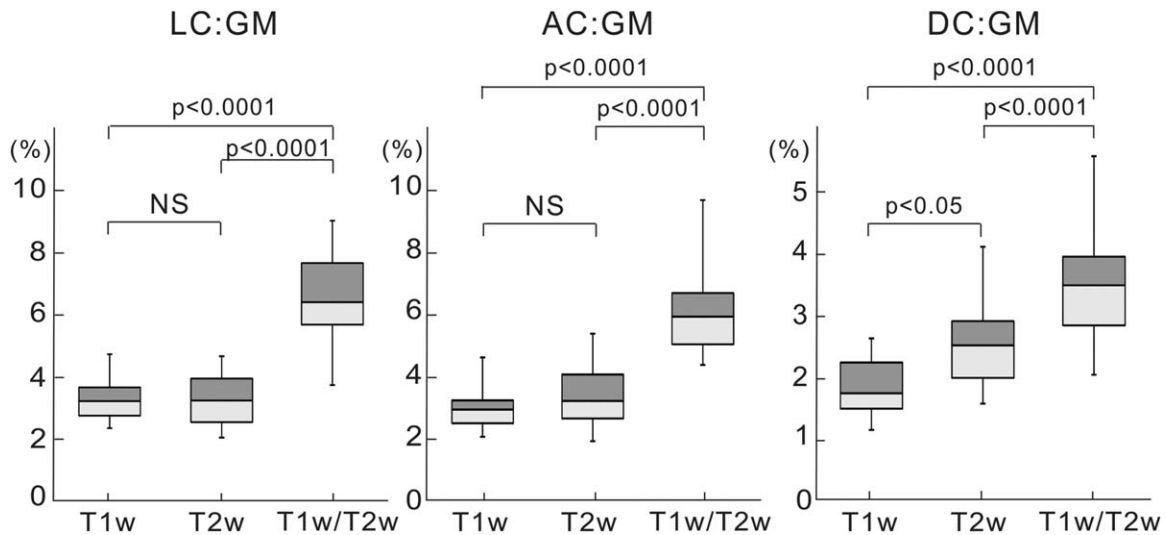


Figure 6. Mean contrast among all segments at each location for each subject. A paired t-test revealed a significant difference in contrast between the ratio (T1w/T2w) and the T1w or T2w image for all locations ($P < 0.0001$ with Bonferroni correction).

Effect of Age on the Signal Intensity

Figure 7 shows that the signal intensity of the T1w/T2w ratio images was inversely related to age at all locations ($r = -0.60$ ($P < 0.005$) to -0.42 ($P < 0.05$)). In

contrast, no significant relationship was found between the signal intensity and age for the T1w or T2w images, except the GM signal in the T1w images.

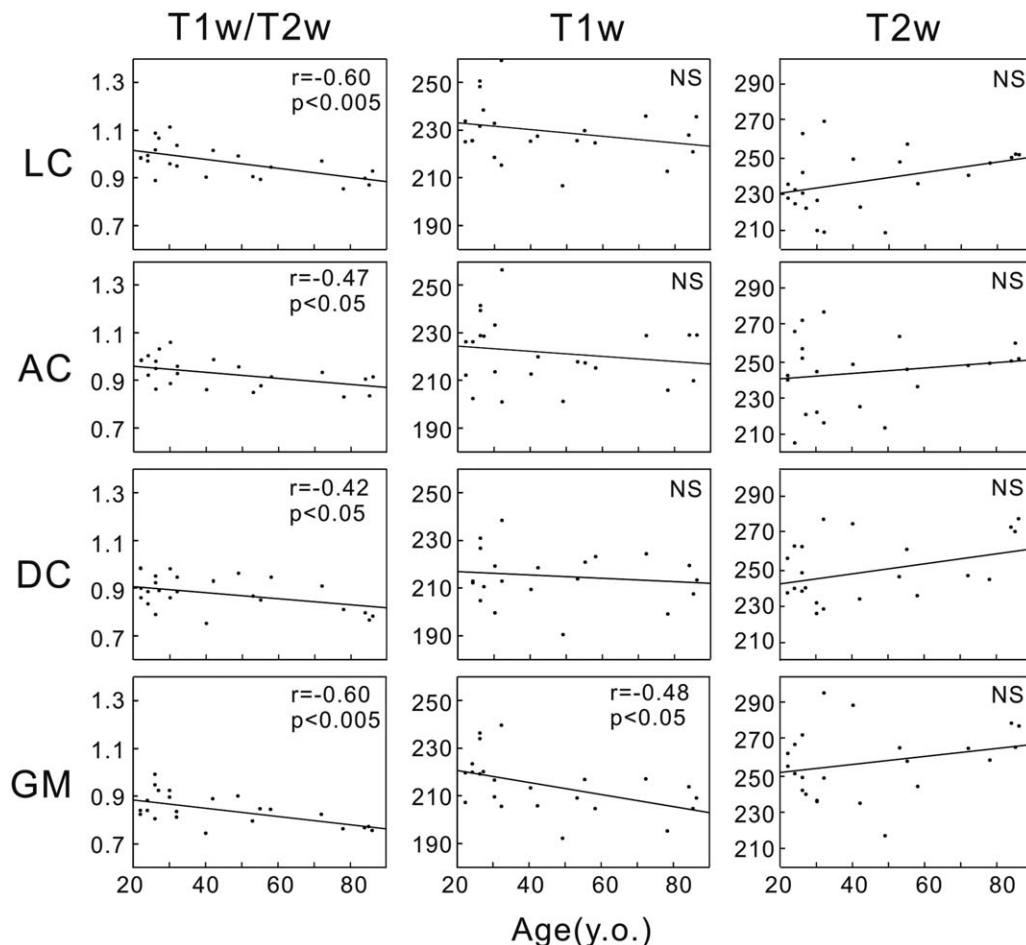


Figure 7. Signal intensity change with age at each location. For all locations, the signal intensity for the T1w/T2w ratio images at the C4 level inversely correlated with age. Note that the inter-individual variance for the same age range is substantially reduced in the T1w/T2w ratio images compared with the T1w or T2w signal intensity.

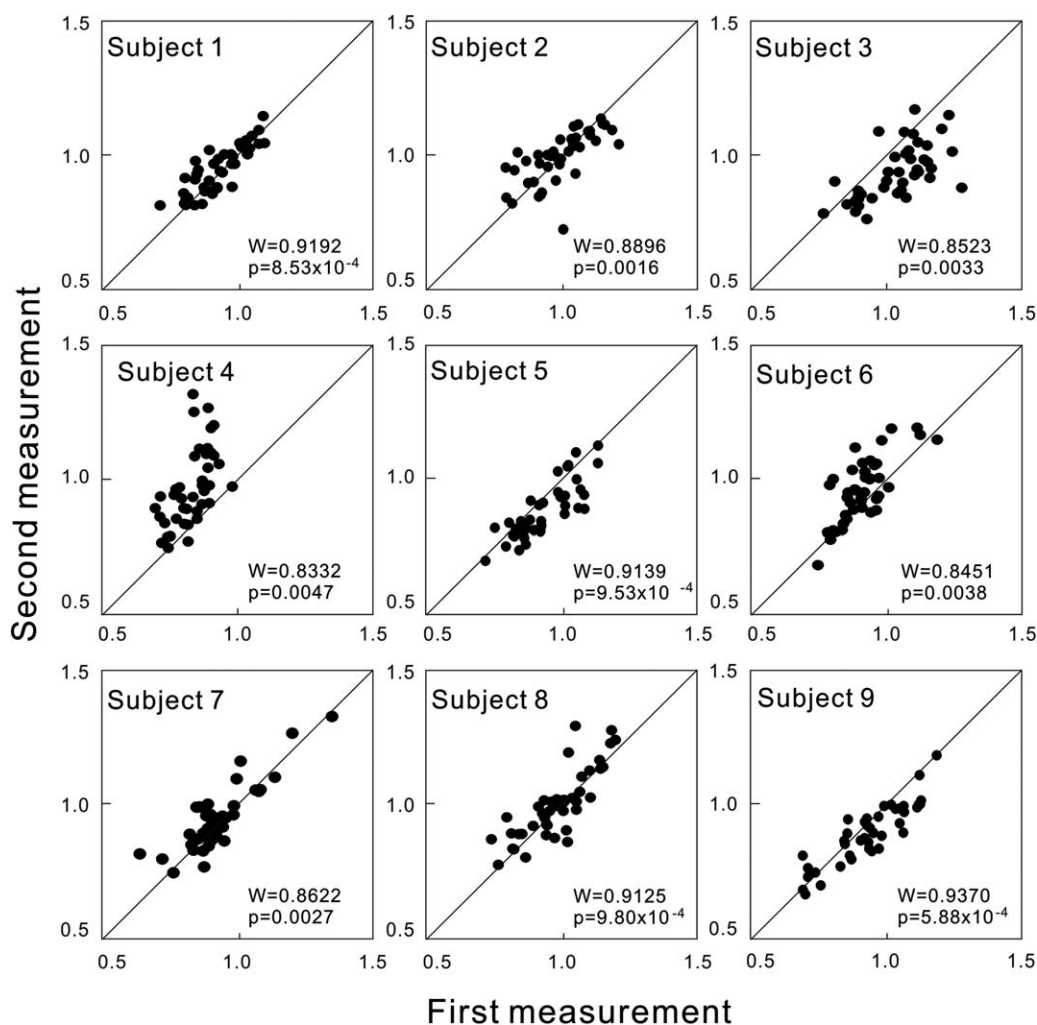


Figure 8. Reproducibility of the signal intensity measurement with the T1w/T2w ratio image. The reproducibility of the signal intensities in the T1w/T2w ratio images of the first and second measurement at six locations (signal intensity of the bilateral AC, LC, single DC, and mean signal intensity of the bilateral GM) at seven segments in nine subjects. Kendall's W coefficients of concordance were all greater than 0.8 and the P-values were all significant.

Reproducibility of the Signal Intensity Measurement

Figure 8 shows the reproducibility of the signal intensities in the T1w/T2w ratio images of the first and second measurement at six locations (signal intensity of the bilateral AC, LC, single DC, and mean signal intensity of the bilateral GM) at seven segments in nine subjects. Kendall's W coefficients of concordance were all greater than 0.8, and the P-values were all significant.

Signal Intensity Change in Spinal Diseases

Figure 9 shows the signal intensities (red line) in the T1w/T2w ratio image for the 39-year-old MS subject. Significantly low intensities were seen continuously in the one to two vertebral levels from the normal range between the broken lines, as calculated using the values from the controls. In contrast, the 77-year-old CS myelopathy subject showed a rather sharp decrease in signal intensity within a localized segmental level at several different segmental locations (Fig. 10).

Because the signal intensity was inversely related to age (see Fig. 7), the normal range for a 77-year-old subject was estimated using linear regression of the values used in Figure 9. For both subjects' images, the spatial extent of the lesions was seen more clearly in the T1w/T2w ratio images than in the T2w images.

DISCUSSION

In this study, we showed that the contrast in the T1w/T2w ratio images was approximately twice that of the T1w or T2w images, and that the signal intensity of the ratio image was inversely related to the subject's age. The results, however, depends on the signal-to-noise ratio (SNR) of the T1w and T2w images and the precise co-registration of both images. Glasser and Van Essen registered T2w images to T1w images using FSL's FLIRT (20), which is considered to be the standard processing tool in brain functional MRI studies. Here, we set the voxel size at $1 \times 1 \times 2$ mm to optimize the SNR and spatial resolution considering a longitudinal orientation of the spinal cord. Because no standard acquisition software or MR

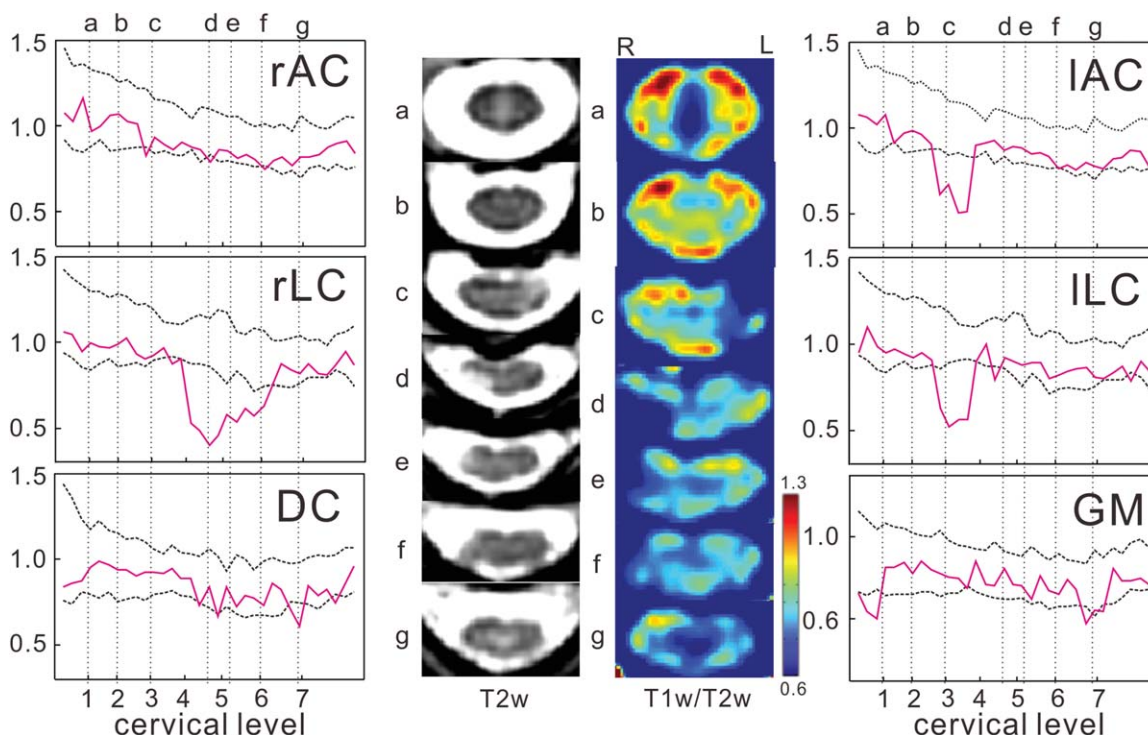


Figure 9. T1w/T2w ratio image at each location of multiple sclerosis patient. Slice number “c” deviates from control data at left AC and LC. Slice number “d,e” deviates from control data at right LC, however, DC falls in the range of control data.

pulse sequences for spinal cord imaging were used for spinal cord image registration, we used a SOMI brace (modified for MRI) to reduce body motion during the image acquisition, and the reproducibility of the signal intensity measurement was confirmed. Although we measured the contrast between WM and GM, the

contrast increase does not rely on the exact localization of the WM and GM, meaning that the same discussion can also be made with two locations within the same tissue. Thus, the lower spatial resolution of the image to discriminate GM and WM is not a critical issue in the argument for the contrast increase with

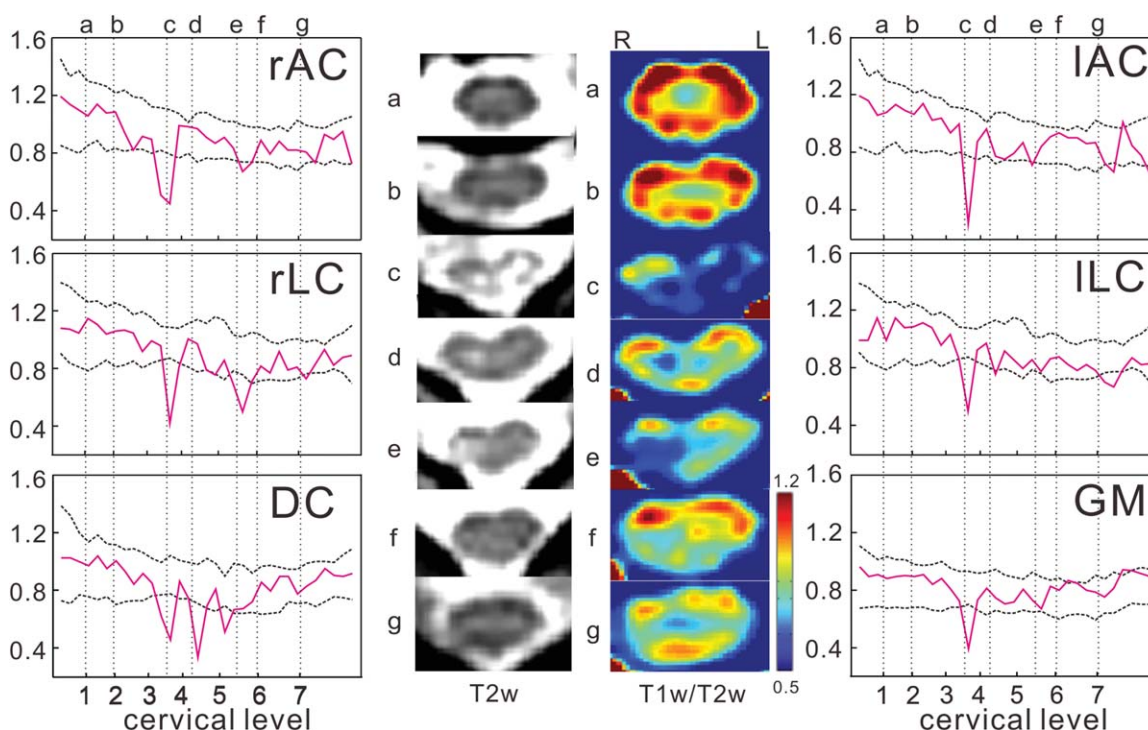


Figure 10. T1w/T2w ratio image at each location of cervical spondylotic myelopathy patient. Slice number “c” deviates from control data at every location, which is required for establishing accurate correlations with MRI parameters.

the T1w/T2w ratio; however, the reduction factor of SENSE was important to increase the SNR with a limited acquisition time.

The measured contrast decreased at the lower segmental levels for all images. The reason for this is unknown, but it might be related to the WM areal fraction (WMAF). The WMAF decreases as the cervical level shifts caudally (from C2 to C7) (17). This can worsen the GM discrimination (that is, WM signal contamination to GM), which results in reduced contrast. A similar tendency has been shown for the change in the myelin water fraction with the cervical segment, which also seems to be due to the WMAF (15). Another reason for the lower contrast in the lower cervical segment might be larger body motion (possibly related to respiration) compared with the upper segments. Moreover, we could not reduce possible artifacts due to CSF pulsation, which could be larger in the lower segments. Because these artifacts could not be eliminated by the image acquisition protocol and device, development of postprocessing software for spinal cord imaging with higher spatial resolution and faster image acquisition is necessary.

Even though our artifact reduction may not be optimal, we successfully showed that inter-individual differences in the signal intensity were eliminated by using the T1w/T2w ratio, and a clear relationship was seen between the signal intensity and age. One possible reason for the correlation with age is that the variance in signal intensity was reduced by cancelling the effect of body size and spinal cord location relative to the receiver coil. In the aging spinal cord, the density of nerve fibers decreases; consequently, the T1w/T2w ratio intensity might be reduced. Previous anatomical and morphological studies indicated a drop in the number of myelinated fibers (21) and decreased fractional anisotropy with age (10). It suggests that the age-related changes in myelin content and cell morphology are unlikely to appear on conventional T1w or T2w imaging. By contrast, the contrast enhancement in the T1w/T2w ratio images may reflect the myelin content and cell morphology by canceling out artifacts (18). The T1w/T2w ratio image is not always related to the myelin content; however, it is related to the pathological time course.

Our findings raise the possibility that one can numerically assess signal intensity change due to pathological changes in the spinal cord by using the signal intensity in T1w/T2w ratio images. Indeed, we found a significant decrease (exceeding -2 SD of the normal subjects' distribution) of the signal intensities in the lesion areas; both MS and CS myelopathy changes were significantly below the normal range, which might be due to the chronic stage of the disease in both subjects. Repetitive measurements of the signal intensity at the same lesion location may be useful to assess the clinical course of spinal cord diseases because the signal intensity of T1w/T2w ratio images should be stable unless pathological changes occur, as long as the same MRI scanners and acquisition parameters are used.

We acknowledge several limitations. First, the signal intensity in the ratio images is not always related to

the myelin content in pathological lesions. When the myelin content decreases in a lesion, the T1w signal should decrease and the T2w signal should increase, resulting in decreased signal intensity in the ratio images. However, the actual T1w and T2w signal changes are quite variable (4,8,22) and depend on the pathological time course, even within the same disease (9). Second, although we observed a significant increase in contrast as expected in the T1w/T2w ratio images, CNR may not increase as much. This is because the T1w/T2w ratio images were not generated from independently measured signals, but from the values derived from two measured values. According to the propagation of error law, the division of two measured values increases the error distribution and decreases the SNR, even if the two measured values are not correlated with each other, which diminishes the increase in the CNR by the increase in the contrast. Third, the same MRI scanners and acquisition parameters should be used to assess the clinical course of spinal cord changes.

In conclusion, we show that the contrast of T1w/T2w ratio images was approximately twice that of T1w and T2w images, and inter-individual differences were eliminated in the ratio images. These findings suggest that the T1w/T2w ratio image represents a useful clinical protocol to numerically assess spinal cord image signal intensity.

REFERENCES

1. Ross JS. Newer sequences for spinal MR imaging: smorgasbord or succotash of acronyms? *AJNR Am J Neuroradiol* 1999;20:361-373.
2. Maier SE. Examination of spinal cord tissue architecture with magnetic resonance diffusion tensor imaging. *Neurotherapeutics* 2007;4:453-459.
3. Meindl T, Wirth S, Weckbach S, Dietrich O, Reiser M, Schoenberg SO. Magnetic resonance imaging of the cervical spine: comparison of 2D T2-weighted turbo spin echo, 2D T2-weighted gradient-recalled echo and 3D T2-weighted variable flip-angle turbo spin echo sequences. *Eur Radiol* 2009;19:713-721.
4. Do-Dai DD, Brooks MK, Goldkamp A, Erbay S, Bhadelia RA. Magnetic resonance imaging of intramedullary spinal cord lesions: a pictorial review. *Curr Probl Diagn Radiol* 2010;39:160-185.
5. Zhang YZ, Shen Y, Wang LF, Ding WY, Xu JX, He J. Magnetic resonance T2 image signal intensity ratio and clinical manifestation predict prognosis after surgical intervention for cervical spondylotic myelopathy. *Spine* 2010;35:E396-E399.
6. Mastronardi L, Elsawaf A, Roperto R, et al. Prognostic relevance of the postoperative evolution of intramedullary spinal cord changes in signal intensity on magnetic resonance imaging after anterior decompression for cervical spondylotic myelopathy. *J Neurosurg Spine* 2007;7:615-622.
7. van Walderveen MA, Kamphorst W, Scheltens P, et al. Histopathologic correlate of hypointense lesions on T1-weighted spin-echo MRI in multiple sclerosis. *Neurology* 1998;50:1282-1288.
8. Green C, Butler J, Eustace S, Poynton A, O'Byrne JM. Imaging modalities for cervical spondylotic stenosis and myelopathy. *Adv Orthop* 2012;2012:908324.
9. Poloni G, Minagar A, Haacke EM, Zivadinov R. Recent developments in imaging of multiple sclerosis. *Neurologist* 2011;17:185-204.
10. Mamata H, Jolesz FA, Maier SE. Apparent diffusion coefficient and fractional anisotropy in spinal cord: age and cervical spondylosis-related changes. *J Magn Reson Imaging* 2005;22:38-43.
11. Biton IE, Duncan ID, Cohen Y. High b-value q-space diffusion MRI in myelin-deficient rat spinal cords. *Magn Reson Imaging* 2006;24:161-166.

12. Cohen-Adad J, El Mendili MM, Lehericy S, et al. Demyelination and degeneration in the injured human spinal cord detected with diffusion and magnetization transfer MRI. *Neuroimage* 2011;55: 1024–1033.
13. MacMillan EL, Madler B, Fichtner N, et al. Myelin water and T(2) relaxation measurements in the healthy cervical spinal cord at 3.0T: repeatability and changes with age. *Neuroimage* 2011;54: 1083–1090.
14. Kozlowski P, Liu J, Yumg AC, Tetzlaff W. High-resolution myelin water measurements in rat spinal cord. *Magn Reson Med* 2008; 59:796–802.
15. Kolind SH, Deoni SC. Rapid three-dimensional multicomponent relaxation imaging of the cervical spinal cord. *Magn Reson Med* 2011;65:551–556.
16. Kaneoke Y, Furuse M, Inao S, et al. Spin-lattice relaxation times of bound water—its determination and implications for tissue discrimination. *Magn Reson Imaging* 1987;5:415–420.
17. Minty EP, Bjarnason TA, Laule C, MacKay AL. Myelin water measurement in the spinal cord. *Magn Reson Med* 2009;61:883–892.
18. Glasser MF, Van Essen DC. Mapping human cortical areas in vivo based on myelin content as revealed by T1- and T2- weighted MRI. *J Neurosci* 2011;31:11597–11616.
19. Pruessmann KP, Weiger M, Scheidegger MB, Boesiger P. SENSE: sensitivity encoding for fast MRI. *Magn Reson Med* 1999;42:952–962.
20. Jenkinson M, Bannister P, Brady M, Smith S. Improved optimization for the robust and accurate linear registration and motion correction of brain images. *Neuroimage* 2002;17: 825–841.
21. Terao S, Sobue G, Hashizume Y, Shimada N, Mitsuma T. Age-related changes of the myelinated fibers in the human corticospinal tract: a quantitative analysis. *Acta Neuropathol* 1994;88:137–142.
22. Ohshio I, Hatayama A, Kaneda K, Takahara M, Nagashima K. Correlation between histopathologic features and magnetic resonance images of spinal cord lesions. *Spine* 1993;18:1140–1149.